Rotational Tunneling of Methane in Metal-Organic Frameworks

An experiment using the NCNR Disk Chopper Spectrometer

Summer School on the Fundamentals of Neutron Scattering
NIST Center for Neutron Research
June 19-23, 2017

Wei Zhou, Nick Butch, and Craig Brown

Abstract

Time-of-flight neutron spectroscopy will be used to examine the local potentials of methane adsorbed in metal-organic frameworks. This experiment illustrates the important phenomenon of neutron scattering from tunneling molecules. We shall discuss all aspects of the experiment, from sample preparation and the choice of instrumental setup through to data treatment and interpretation of results.

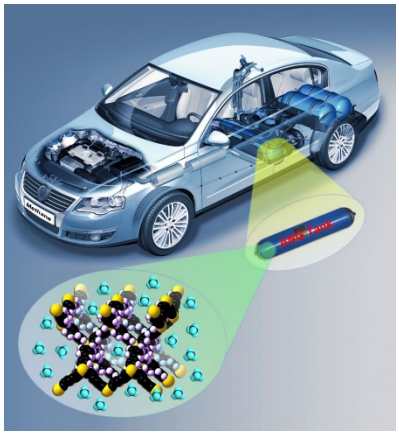

Metal-organic framework material helps with methane storage in vehicles powered by natural gas. (Image credit: Texas A&M Univ.)

I. Introduction

Natural gas, consisting primarily of methane (CH_4), is an excellent fuel that burns cleaner than all other fossil fuels. Recent years have witnessed a rapid increase of newly discovered natural gas reserves worldwide, and a dramatic decrease in the natural gas to gasoline price ratio. Natural gas is thus widely regarded as a "bridge" fuel to help us through the transition from traditional fossil fuels to future clean/renewable energy (*e.g.*, solar energy). Despite its wide application in both industrial and domestic markets, the usage of natural gas in vehicles is rather limited, largely due to its low volumetric energy density under ambient conditions. Currently there is great interest in promoting natural gas for on-board applications [*e.g.*, see the U.S. Department of Energy's research program "Methane Opportunities for Vehicular Energy (MOVE)", http://arpa-e.energy.gov/?q=arpa-e-programs/move], and efficient methane storage technology is actively pursued. Common natural gas storage methods including liquefaction and compression are relatively mature technologies, but they suffer due to the extreme operating conditions (200-300 bar for compressed methane, and 112 K for liquefied methane) and the related energy cost. An alternative technology, which could potentially be safer and cheaper, is to use porous adsorbent materials to help store methane in a fuel tank under relatively mild conditions.

Emerging as a new type of porous material, metal-organic frameworks (MOFs), which consist of metal ions or metal-containing clusters linked by organic ligands through metal coordination bonds, have attracted much attention for their promising applications as adsorbent materials for methane storage (see: *Chem. Soc. Rev.* **2014**, *43*, 5657; *Nature* **2015**, *527*, 357). This is largely because of their unique characteristics: highly crystalline structures, nanometer-sized pores, ultrahigh porosities, and functionalizable pore walls. Thus far, a dozen or so MOFs have been found to exhibit relatively high methane storage capacities, and further efforts are being devoted to the design and synthesis of new MOFs, emphasizing improved methane storage performance. To facilitate this research, it is critical to understand the fundamentals of methane-MOF interactions.

Neutron scattering is an excellent probe for studies of methane adsorption in MOFs. Neutron diffraction measurements can directly reveal where the methane molecules are adsorbed/stored, and neutron spectroscopy can help us investigate the strength of the methane-framework interaction, as we shall see in this experiment. We are going to examine two iconic metal-organic framework materials: MOF-5 (metal-organic framework-5, see *Nature* **1999**, *402*, 273) and UiO-66 (UiO: *University of Oslo*, see *JACS* **2008**, *130*, 13850), whose structures are schematically shown in Figure1. The metal centers in MOF-5 and UiO-66 are Zn_4O and $Zr_6O_4(OH)_4$, respectively, whereas the organic linkers in the two MOFs are the same, namely, benzene-1,4-dicarboxylate (BDC).

Previous neutron diffraction studies have elucidated the methane adsorption sites in these MOFs. In MOF-5, the first and strongest binding sites for methane lie in the so-called "cup" site of the ZnO_4 clusters with the orientation of the methane molecule being well resolved, where one of the CH-bonds is along the 3-fold axis (Fig.2, left). Similarly, methane molecules were preferentially adsorbed in UiO-66 at the "cup" site of the $Zr_6O_4(OH)_4$ metal center (Fig.2, right), with 3-fold local symmetry. Carefully synthesized MOF-5 crystals

can have nearly “perfect” structure, and thus represent a model system to study methane tunneling. In contrast, UiO-66 samples obtained from a typical synthesis route usually contain ~10% linker vacancies, which would make the methane tunneling data analysis more complicated.

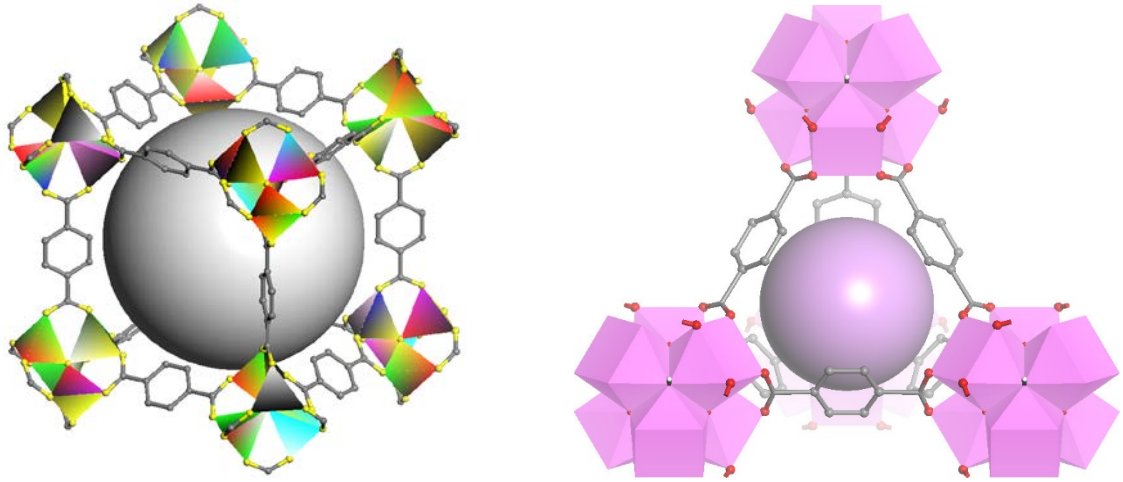

Figure 1. Two metal-organic frameworks studied in this experiment: MOF-5 (left) and UiO-66 (right). The metal-O clusters are plotted as ZnO_4 and ZrO_8 polyhedra. Large spheres at the framework center denote the pores within the MOF structures. Hydrogen atoms on the organic linkers are omitted for clarity.

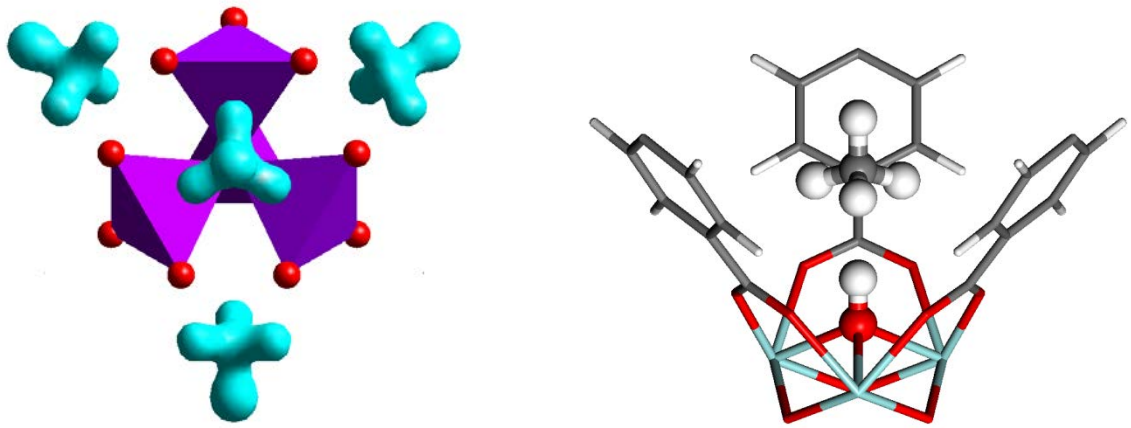

Figure 2. (Left) Excess neutron scattering-length density superimposed with the ZnO_4 clusters of the MOF-5 host structure, indicating the location of cup-sites for the first methane adsorption. (Right) Methane adsorption on the Zr-metal centers in UiO-66. Both were derived from neutron diffraction data.

We will be using the Disk Chopper Spectrometer at the National Institute of Standards and Technology Center for Neutron Research to probe dynamics and the local potential at the methane adsorption site. After reading the background material you should be able to choose an appropriate spectrometer configuration to probe the rotational tunneling or temperature dependent diffusional dynamics present in the methane:MOF system.

The neutron has several properties that enable scattering experiments to measure properties of materials that other techniques can measure with much less precision or not at all. Neutrons with wavelengths on the order of interatomic spacings also possess energies on the same order as those characteristic of phonons and intermolecular interactions; for example, a 1.8 Å neutron has an energy of ~25 meV (~200 cm^{-1}) and speed ~2200 ms^{-1}. This means that structural and temporal information can be measured simultaneously.

The reader is reminded that the scattering of neutrons is usually treated as the sum of two parts, known as *coherent* and *incoherent* scattering. To understand why such a separation is performed recall that the strength of the scattering from nuclei of the same element can vary (and generally does vary) with spin and/or isotopic species. Hence when a neutron is scattered by a collection of nuclei the interference between the different scattered waves is normally neither complete nor completely absent. For this reason the *double differential cross section* $[d^2\sigma/d\Omega d\omega]$, which describes the probability that neutrons are scattered into solid angle $d\Omega$ and energy transfer window $d(\hbar\omega)$, is normally separated into two terms. The first term is the coherent part, which contains all of the interference effects such as Bragg scattering and small angle scattering. The second term is the incoherent scattering, which represents the scattering from individual nuclei and is approximately isotropic. For a single element $[d^2\sigma/d\Omega d\omega]$ can be expressed as

$$\frac{d^2\sigma}{d\Omega d\omega} = \frac{1}{4\pi}\frac{k_f}{k_i}[\sigma_{coh}S(Q,\omega) + \sigma_{inc}S_{inc}(Q,\omega)] \qquad (1)$$

where k_i and k_f are the magnitudes of the initial and final neutron wave vectors, σ_{coh} and σ_{inc} are the coherent and incoherent scattering cross sections, and $S(Q,\omega)$ and $S_{inc}(Q,\omega)$ are the corresponding scattering functions which depend only on the momentum transfer $\hbar Q$ (or wave vector transfer Q) and the energy transfer $\hbar\omega$. (Note that in general Q is a vector but since we shall be working with a powder with cubic crystal symmetry, and no preferred orientation, all that need concern us in this experiment is the magnitude of the wave vector.) The most important incoherent scatterer is hydrogen for which σ_{inc}= 80.3 barns/atom whereas σ_{coh} is only 1.76 barns/atom (1 barn = $10^{-24}cm^2$). Since the incoherent scattering cross section of hydrogen is much larger than those of almost all other nuclei, it is often reasonable (as a first approximation) to neglect the coherent scattering in systems that contain a relatively large fraction of hydrogen atoms.

Can you explain the usefulness of deuteration, given that σ_{coh}(deuterium) and σ_{inc}(deuterium) are 5.6 barns/atom and 2 barns/atom, respectively?

Elastic neutron scattering is scattering with no change in neutron energy, i.e. with $\hbar\omega = 0$. On the other hand, *inelastic neutron scattering* is scattering with a change in neutron energy, i.e. with $\hbar\omega \neq 0$. *Quasielastic neutron scattering* (QENS) is a type of inelastic scattering that involves the Doppler-like broadening of otherwise elastically scattered neutrons due to reorientational or diffusive motions of atoms in the target material. Thus QENS is a special kind of inelastic neutron scattering. In this experiment you will use neutron scattering to perform low energy inelastic measurements on methane tunneling modes and to measure corresponding QENS spectra at higher temperatures.

We shall first describe the samples to be used for the experiment, and the equipment that will be used to bring them to the desired measurement conditions (methane concentration and temperature). The next section provides a brief discussion of the spectrometer as well as matters to be considered in choosing the incident wavelength for this experiment. We then describe the reduction of the data to obtain the scattering function, and we follow with some words about the scattering that is expected for these measurements. This then sets the scene for the analysis and discussion of the experimentally measured scattering function.

II. The samples

We have synthesized somewhat more than 2 grams of deuterated MOF-5, and roughly 1 gram of deuterated UiO-66. In preparation for the summer school, each sample will have been loaded into a vanadium pressure cell with a valve and gas-line attached. Before the start of each group's experiment, we will have mounted and cooled one of the samples in a low temperature environment (helium cryostat or closed cycle refrigerator) and selected background measurements will have been completed. The group's experiment may or may not include bare samples in addition to the samples loaded with methane using a home-made gas loading system. Through the night we shall collect data at temperatures and wavelengths decided by the group.

Why do we typically use aluminum for sample containers and cryostat windows?

Apart from indium, what materials might be used to seal sample containers?

To reduce the data we will also need a detector normalization file obtained using a sample of vanadium metal, plus a run with the beam closed (a type of background, or "dark count"). These runs will have been performed before the start of the summer school since there will not be time to complete them once the school is underway.

Why do we use vanadium to normalize the data from different detectors? Hint: σ_{coh}= 0.02 barns/atom, σ_{inc}= 5.19 barns/atom.

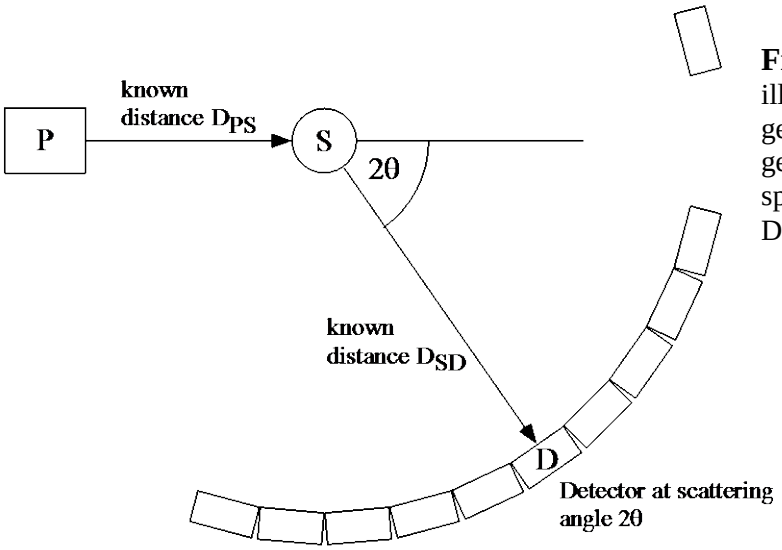

Figure 3. A schematic illustration of the scattering geometry for a direct geometry time-of-flight spectrometer such as the DCS.

III. The spectrometer

We shall be performing this experiment using the Disk Chopper Spectrometer (DCS), which is a so-called "direct geometry" (fixed incident energy) time-of-flight spectrometer. In this type of instrument (figure 3) bursts of monochromatic neutrons strike the sample at equally spaced times. The energies of the scattered neutrons are determined from their arrival times at the detectors, since we know when the pulses were created as well as the distances D_{PS} from the pulsing device to the sample and D_{SD} from the sample to the detectors. There are two ways to produce a monochromatic pulsed beam at a steady state neutron source. One method is to use a single crystal to monochromate the white beam and a mechanical "chopper" to pulse it; the other method is to use multiple choppers, such as the seven (!) choppers of the DCS.

> A monochromatic pulsed beam of neutrons can in principle be created using two choppers. How does that work? Can you think why more than two choppers might be needed and/or desirable?

Given the initial and final energies of the neutrons, E_i and E_f, the energy transfer $\hbar\omega = E_i - E_f$ is trivially obtained. Knowing the scattering angle 2θ we can also calculate the magnitude of the momentum transfer to the sample, $\hbar Q$:

$$(\hbar Q)^2 = 2m_n\left[E_i + E_f - 2\sqrt{E_i E_f}\cos 2\theta\right] \qquad (2)$$

where m_n is the mass of the neutron. (This follows from the definition $\vec{Q} = \vec{k_i} - \vec{k_f}$ and the relationship between the magnitude of a neutron's wave vector, k, and its energy E: $E = h^2k^2/2m_n$.)

The data acquisition system separately accumulates neutron counts for each of the 913 DCS detectors. Furthermore the time between pulses, T, is normally divided into 1000 time channels of equal width $\Delta t = 0.001T$ and each neutron event in a given detector is stored in one of these time channels according to its time of arrival at the detector. Thus the data acquisition system generates a two-dimensional array of counts I(i,j) as a function of detector index i and time channel index j. This array is accumulated in a "histogramming memory" which is resident in the data acquisition computer. At the end of each run cycle the array is saved, along with other pertinent information, to the hard disk of the instrument computer.

With the sample environment mounted on the spectrometer, we can control and monitor the temperature remotely, but care must be taken not to exceed 110 K so that methane does not desorb from the sample. The choice of incident wavelength is critical to the experiment and several factors must be considered. These include intensity at the sample (which peaks, remaining roughly constant, between ~2.5 and ~4.5 Å, see Appendix A), the width of the elastic energy resolution function (which roughly varies as $1/\lambda^3$), the available Q range (which varies as $1/\lambda$), and concerns about "frame overlap" problems. A related consideration is the available range in sample energy gain (neutron energy loss).

What is the maximum theoretical sample energy gain that can be measured when the incident energy is E_i, and how long would it take to measure the intensity of neutrons scattered with this change in energy?

Overnight you will be collecting data. To this end, you will need to define a "sequence" consisting of several "runs" plus at least one change of sample temperature and probably wavelength. Each run is divided into a set of "cycles" that are of defined lengths of time. At the end of each cycle the temperature is recorded and the data are backed up to the disk. Having defined the runs we shall start the overnight sequence of measurements. Next day we shall stop the measurements and start into the data reduction.

In the experimental runs we shall collect intensity histograms I(i,j) for the sample at at least two temperatures. Using previously acquired intensity histograms for a vanadium sample and for a "dark count" run with the beam shutter closed, we shall reduce the data to obtain the scattering function $S(Q,\omega)$, and various cuts in both Q and ω.

IV. Data reduction

In this section we shall simply indicate some of the more important steps in the data reduction process. We shall go into greater detail in our discussions at the time that the data reduction takes place.

In each experiment, the measured scattering includes intrinsic scattering from the sample plus background scattering intensity. Before we do any data analysis we need to subtract a time-independent background from each of the runs.

Where does the time independent background come from?

Neglecting effects such as self-shielding and multiple scattering the scattering in detector i and time channel j may be related to the corresponding double differential cross section $[d^2\sigma/d\Omega dt]_{ij}$ (note that this is per unit time, not energy) in the following fashion:

$$I(i,j) = \frac{I_{BM}}{\eta_{BM}} \cdot \left[\frac{d^2\sigma}{d\Omega dt}\right]_{ij} \Delta\Omega\Delta t \cdot N_m \cdot \eta_{ij} \qquad (3)$$

where $\Delta\Omega$, the solid angle subtended by detector i, and Δt, the width of time channel j, are (for these measurements) presumed to be independent of i and j respectively, N_m is the number of sample molecules in the beam, η_{ij} is the efficiency of detector i for neutrons detected in time channel j, and I_{BM} and η_{BM} are respectively the counts and the efficiency of the beam monitor (situated upstream of the sample).

Since we are not trying to extract an absolute cross section we can neglect the multiplicative constants in the above equation, but we should not ignore the detector efficiency function η_{ij}. Since all of the detectors are to first order identical it is not unreasonable to treat η_{ij} as the product of two terms, a function η_{i0} which represents the efficiency of detector i for elastically scattered neutrons and a detector-independent function f_j that describes the energy dependence of the efficiency of the detectors. The correction for differences in detector response, i.e. the determination of η_{i0}, is performed using the results of a measurement with a vanadium sample.

The correction of the data for the energy dependence of the efficiency is achieved by calculation, knowing the various factors that affect the probability that a neutron is absorbed within a detector.

What are these factors?

To improve statistics, we may define several detector groups, each of which includes detectors within a specified range of angles. The differential cross section $[d^2\sigma/d\Omega dt]$ for all detectors in a group will be summed and divided by the number of detectors in the group. Having obtained a quantity proportional to $[d^2\sigma/d\Omega dt]$ we must now compute $[d^2\sigma/d\Omega d\omega]$ and finally $S(Q,\omega)$. Since a neutron's energy E is related to its time-of-flight t over a fixed distance as $E \propto t^{-2}$, it follows that $dE \propto t^{-3}dt$. Hence

$$\frac{d^2\sigma}{d\Omega d\omega} \propto \frac{d^2\sigma}{d\Omega dE_f} = \left[\frac{d^2\sigma}{d\Omega dt}\right]\left(\frac{dt}{dE_f}\right) \propto \left[\frac{d^2\sigma}{d\Omega dt}\right] t^3 \qquad (4)$$

To obtain $S(Q,\omega)$ we simply divide by k_f (see eq. 1). Equivalently we multiply by another factor of t.

If a system in thermodynamic equilibrium can exist in a number of thermodynamic states and we consider two such states separated by an energy difference $\hbar\omega$, the probability that the system is in the lower energy state is greater by a factor $\exp(\hbar\omega/kT)$ than the probability that it is in the higher energy state. From this it can be shown that for systems in thermodynamic equilibrium the scattering function $S(Q,\omega)$ satisfies the so-called "detailed balance" relationship: $S(-Q,-\omega) = \exp(-\hbar\omega/kT)S(Q,\omega)$. Since we shall be fitting the data to a theoretical form that is symmetric in $\hbar\omega$ we shall first "symmetrize" the experimental $S(Q,\omega)$ by multiplying it by $\exp(-\hbar\omega/2kT)$.

Is symmetrization of $S(Q,\omega)$ likely to be a larger effect at low or high temperatures?

Having reduced the experimental data to a symmetrized scattering function it is time to relate the results to theory.

V. Theory

Consider pure methane. In the phase II crystal structure there are actually two different types of methane molecular environments below T = 20 K. These molecules show two kinds of rotational excitations: 75% of the molecules are orientationally ordered lying in the deep minima of a strong potential, while the other 25% are orientationally disordered. The high resolution neutron scattering spectra comprises of tunneling lines at 75 μeV and 145 μeV with a librational feature at 1.07 meV (figure 4(a)) [Asmussen]. Much research has been performed to measure and understand the dynamics of tetrahedral molecules in various environments. Rotational wave functions can be constructed considering the tetrahedral symmetry of the CH_4 molecule with the corresponding total spin of I=2 (ortho), I=1 (meta) and I=0 (para) having representations A (five times one-fold degenerate), T (three times triply degenerate) and E (one time doubly degenerate), respectively. The rotational levels of the hindered rotor molecules are shifted strongly as compared with the free rotor molecules (figure 4(b)) and we can immediately see that the free rotor is responsible for the peak above 1 meV, while the low energy features arise from the tunneling multiplet that occurs due to wavefunction overlap between adjacent deep potential minima. (Note that A↔E transitions are forbidden since they require a nuclear spin change of 2.) In addition to the classically forbidden rotations, there are classical librational motions of the molecule within the potential minimum. These give rise to features above 5 meV.

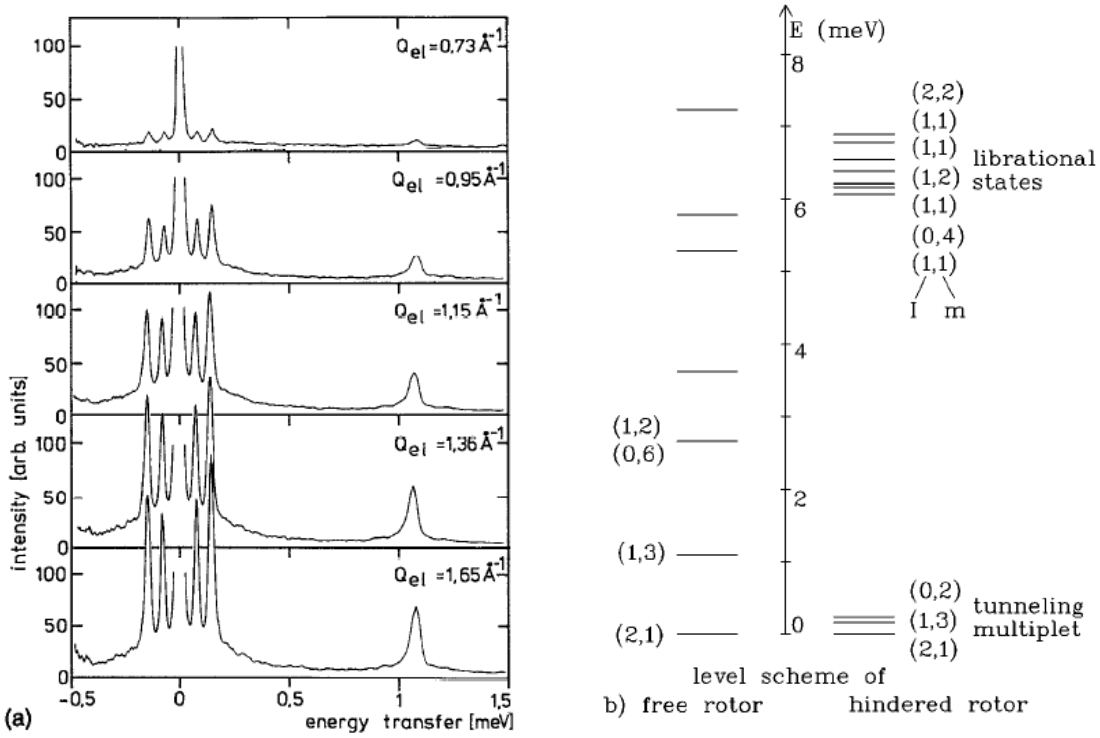

Figure 4. (a) Momentum transfer dependence of the neutron transitions of phase II methane. [Asmussen]. Data were taken on IRIS with the Graphite (002) reflection. (b) Rotational level scheme of methane in solid phase II (after Grieger). Parenthesis (*I*,*m*) denotes the total nuclear spin *I* and the multiplicity *m* of the levels. The multiplicity of the rotational states is *m*(2*I*+1).

In general, there are 9 possible transitions between energy levels for a regular tetrahedral molecule in a potential field that has no specific symmetry. These are shown in Figure 5. However in a symmetric field this number is much reduced and the energy level diagram and tunneling spectra are simplified. For a tetrahedral molecule in a tetrahedral (cubic) field, the T levels are degenerate and hence only two transitions (A↔T and T↔E) are observed as shown above for orientationally ordered methane.

In the current case we need to consider a tetrahedral molecule in a trigonal field, since that is the symmetry of the first methane adsorption site in MOF-5/UiO-66. In this case Huller constructed an energy level scheme which is controlled by two matrix elements, *h* and *h4* (see Huller). These two variables can then be related to the barriers to rotation about both the three equivalent three-fold axes and the unique direction through the center of the cup site.

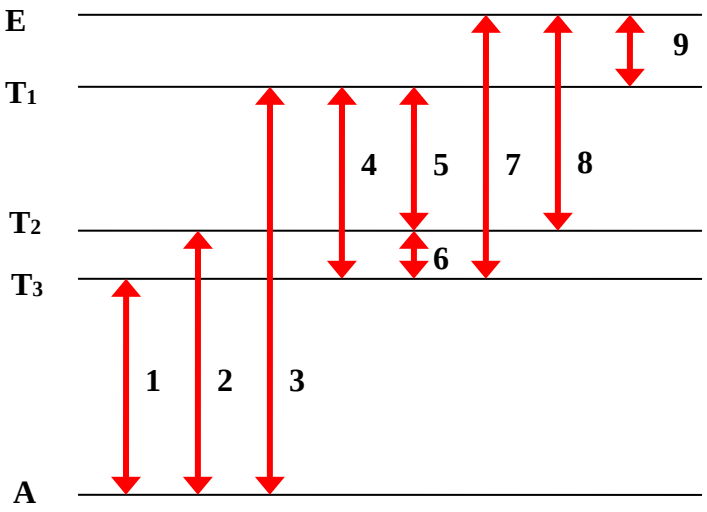

Figure 5.
A schematic illustration of the possible tunneling transitions for a general tetrahedral molecule.

The matrix elements are related to the barrier to rotation about the specified axes and the relative intensities may be arrived at through a lengthy set of integrals (see Huller). For the specific case of a tetrahedral molecule in a trigonal symmetric field, the transitions 1 through 5 have relative ratios 10:5:2:8:4. Further, the spherical average of the Q-dependence has been shown to be related to a series of spherical Bessel functions [see Press].

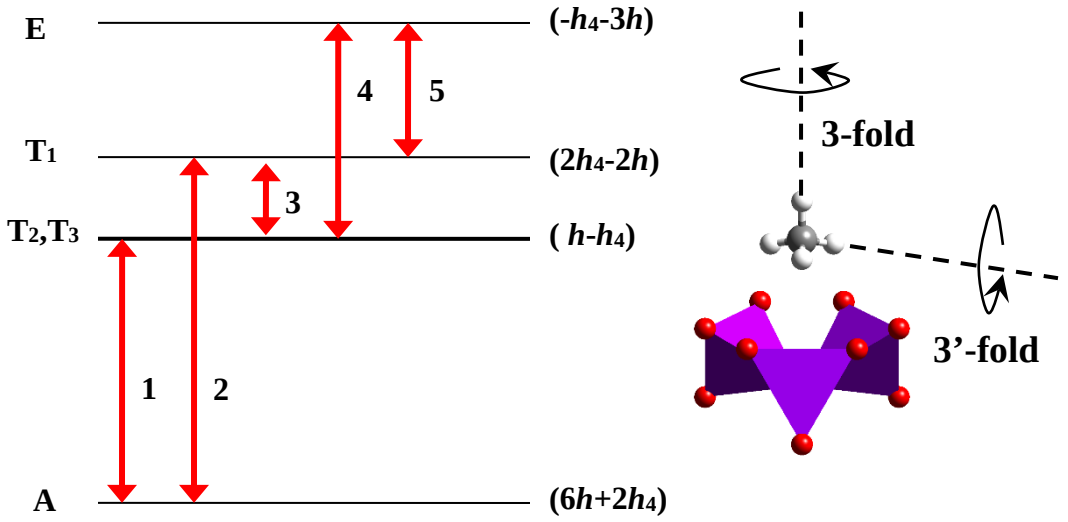

Figure 6. A schematic illustration of the tunneling transitions for a methane molecule in a trigonal field as expected for the first adsorption site in MOF-5 (right). The energy level for each manifold is given as a function of the matrix elements h and h_4.

Upon heating the MOF-CH_4 complex to temperatures up to 110 K, the populations of the methane rotational levels gradually redistribute according to Boltzmann statistics and ultimately there is enough energy in the system to overcome the classical barrier to rotation and a quasielastic feature will develop in the spectra.

Most quasielastic experiments are performed on systems that predominantly scatter neutrons incoherently. The incoherent scattering function is the space and time Fourier transform of the *self-correlation function* $G_s(\vec{r},t)$ which (classically) represents the probability that a particle that was at the origin at time t = 0 is at position $\vec{r}$ at time t.

> Use a similar definition to relate the coherent scattering function to a (different) space-time correlation function. Why is it easier to formulate models of atomic motion using incoherent scattering?

A common way of expressing $S_{inc}(\vec{Q},\omega)$ is in terms of the *intermediate self scattering function* $I_s(\vec{Q},t)$, which is the space Fourier transform of $G_s(\vec{r},t)$:

$$S_{inc}(\vec{Q},\omega) = \frac{1}{2\pi}\int I_s(\vec{Q},t)e^{-i\omega t}dt \tag{5}$$

An illustrative model for $G_s(\vec{r},t)$ (though inappropriate in the context of the present experiment) is that of simple Brownian diffusion, where times of observation are much longer than typical times between collisions. Fick's Law governs this type of diffusion:

$$\frac{\partial}{\partial t}G_s(\vec{r},t) = D\nabla^2 G_s(\vec{r},t), \tag{6}$$

where D is the diffusion constant. A solution to this equation is given by a self-correlation function of the form

$$G_s(\vec{r},t) = \frac{\exp(-r^2/4Dt)}{(4\pi Dt)^{3/2}}, \tag{7}$$

the space Fourier transform of which is

$$I_s(\vec{Q},t) = \exp(-Q^2Dt). \tag{8}$$

Since this represents an exponential decay in time, the time Fourier transform yields a Lorentzian lineshape:

$$S_{inc}(\vec{Q},\omega) = \frac{1}{\pi}\left[\frac{DQ^2}{(DQ^2)^2+\omega^2}\right] \tag{9}$$

that is centered at zero energy transfer and has a full width at half maximum height (FWHM), Γ, given by

$$\Gamma = 2DQ^2. \tag{10}$$

In the current situation, we might expect that the methane undergoes numerous types of reorientation: three fold jumps about the 'unique' axis; rotational diffusion about the 'unique' axis; isotropic jump reorientation between all four sites; preferred jump

reorientation between pseudo-equivalent sites; or isotropic rotation on a sphere. These are not the only possibilities and complications may arise if the rotational motion couples with translational motions.

To simplify the analysis, we will assume an isotropic rotational diffusion model and work through to the expected characteristics of the scattering law. To first order, the rotation of methane can be considered as the diffusion of four rigidly coupled protons at radius R=1.093 Å from the center of mass. In a classical treatment the angular motion of each molecule satisfies Fick's Law and a powder average can then be expressed as a delta function and a sum of Lorentzians:

$$S_{incc}^{rot}(\vec{Q},\omega) = A_0(Q)\delta(\omega) + \sum_{\ell=1}^{\infty}(2\ell+1)\, j_\ell^2(\vec{QR})\frac{1}{\pi}\left[\frac{\tau_l}{1+\omega^2\tau_l^2}\right] \qquad (11)$$

where $A_0(Q) = J_0^2(QR)$ is often called the Elastic Incoherent Structure Factor (EISF).
The correlation time (or equivalently, twice the reciprocal of the FWHM) is related to the diffusion constant D_R through

$$\tau_\ell = \frac{2}{\Gamma} = \frac{1}{\ell(\ell+1)D_R} \qquad (12)$$

and j_ℓ is a spherical Bessel function. Note that the FWHM is Q independent.

References:
Asmussen B., J. Chem. Phys (1992) 97, 1332.
Press W., *Single-Particle Rotation in Molecular Crystals*, Springer Tracts in Modern Physics, Vol. 92, Springer, Berlin, 1981.
Huller, Phys. Rev. B. (1977) 16, 1844.
Grieger, J. Chem. Phys. (1998) 109, 3161.
Smalley M.V., Mol. Phys. (1981) 44, 533

VI. Data analysis

As mentioned earlier, the MOF-5 sample has a nearly defect-free crystal structure, representing a model system for tunneling study, and thus the corresponding data analysis should be relatively straightforward. We will work on MOF-5 data first, and then look into the data for UiO-66, which is complicated because of structural defects.

We will take a few detours on the route to obtaining a symmetrized form of the experimental scattering function, $S(Q,\omega)$. We will sum data to obtain a view of the powder diffraction and we will also sum to obtain a generalized vibrational density of states that we will then briefly compare to the expected librational features.

The next step will be to fit the $S(Q,\omega)$ data in the tunneling regime as a function of Q. We suggest that you try fitting each Q group to a series of phenomenological Gaussians and possibly a background function. Extract the fitted parameters.

Following the method of Smalley *et al.*, we can then use the following figure of tunnel splitting (figure 7) to derive the rotational barriers (given that this plot was obtained with a mean parameter $\tilde{A}$ =-3.8*B*). Note that the rotational constant, *B*, for methane is 0.656 meV. Using the relationships $V = -\frac{8}{9}A_3 - \frac{4\sqrt{15}}{9}\tilde{A}$ and $V' = -\frac{8}{9}A_3 + \frac{4\sqrt{15}}{27}\tilde{A}$, we can extract rotational barriers for the unique and other three-fold axes, V and V', respectively.

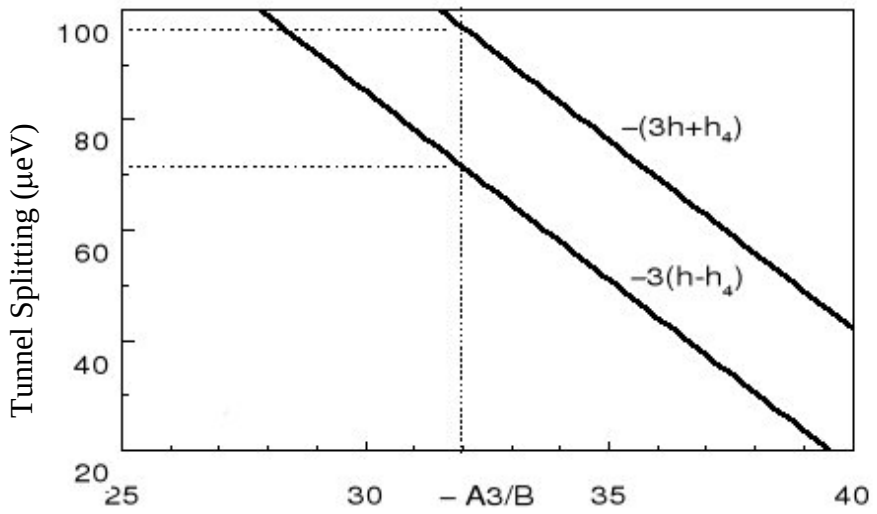

Figure 7. Tunnel splitting parameters as a function of the 'A_3' parameter.

(1) How well do the Gaussians fit?
(2) Assign the features to the rotational transitions for a tetrahedron in a trigonal field
(3) Do the ratios of intensities agree with expectations?
(4) Sum the rotational transitions at each Q. How does this compare with the expected form factor?
(5) Calculate values for *h* and h_4.
(6) Estimate the barriers to rotation about the hard and soft axes.
(7) Methane on graphite has values of 25 meV and 21 meV, respectively. Comment.

If you have taken data at higher temperatures, use the isotropic rotational diffusion model described in the previous section (i.e. an elastic delta function and just *one* broader Lorentzian) to fit the 'empty sample' background subtracted data as a function of Q. In an actual experiment the scattering function is broadened with the instrumental resolution function so the model function must be numerically convoluted with the instrumental resolution function. Having fitted the experimental data to the model, the next step is to make plots of the Lorentzian line parameters as functions of Q.

(8) How well does the single Lorentzian fit?
(9) How do the Lorentzian parameters behave?
(10) Can you extract a rotational diffusion constant or correlation time?
(11) If you have access to other temperatures, can you extract an activation energy?
(12) By taking a ratio of elastic to total scattering and hence extracting A_0, can you fit the expected functional form of the Bessel function?
(13) Does the methane perform isotropic rotational diffusion? Comment.

VII. Concluding remarks

In section V we discussed a scattering function that corresponds to a very simple model of rotational diffusive motion. The situation is more complicated when a system displays more than one type of diffusive motion, or multiple rotational axes. If the various motions are uncoupled, the intermediate scattering function is a product of the individual intermediate scattering functions so that the scattering function is a convolution of the scattering functions for the individual motions. The situation simplifies considerably if additional motions occur on very different time scales. Motions that are much slower than the time scale represented by the instrumental resolution show up as elastic scattering. On the other hand motions that are much faster give rise to an essentially flat background. Different instruments, with different dynamical windows and different resolution capabilities, are needed to observe such motions. For example motions that are too slow to see using the DCS may well show up if the sample is put on the backscattering spectrometer HFBS. Conversely motions that are fast by DCS standards can usefully be studied using the filter analyzer neutron spectrometer (FANS).

VIII. General references

- G.E. Bacon, "*Neutron Diffraction*", Clarendon Press, Oxford (1975).
- M. Bée, "*Quasielastic Neutron Scattering*", Adam Hilger, Bristol (1988).
- R. Hempelmann, "*Quasielastic Neutron Scattering and Solid State Diffusion*", Clarendon Press, Oxford (2000).
- S.W. Lovesey, "*Theory of Thermal Neutron Scattering from Condensed Matter*", Clarendon Press, Oxford (1987).
- G.L. Squires, "*Introduction to the Theory of Thermal Neutron Scattering*", Cambridge University Press (1978), republished by Dover (1996).

Appendix A. Instrument Characteristics for the Disk Chopper Spectrometer

(http://www.ncnr.nist.gov/instruments/dcs)

The white beam from the cold neutron source is cleaned of high energy neutron and gamma ray contamination using an "optical filter". This is basically a bent guide which ensures that there is no line of sight from the source to points beyond the local shutter. A cooled graphite filter removes short wavelength (~0.5 Å) neutrons that remain in the beam, permitting measurements at wavelengths down to roughly 1.5 Å.

A clean, pulsed, monochromatic neutron beam is produced using seven disk choppers. Chopper speeds may be varied from 1200 to 20000 rpm. The pulsing and monochromating choppers have three slots of different widths. In principle this permits three choices of intensity and resolution at a given wavelength and master chopper speed.

The measured intensity at the sample is reproduced below. Red and blue points correspond to measurements using different chopper slot widths.

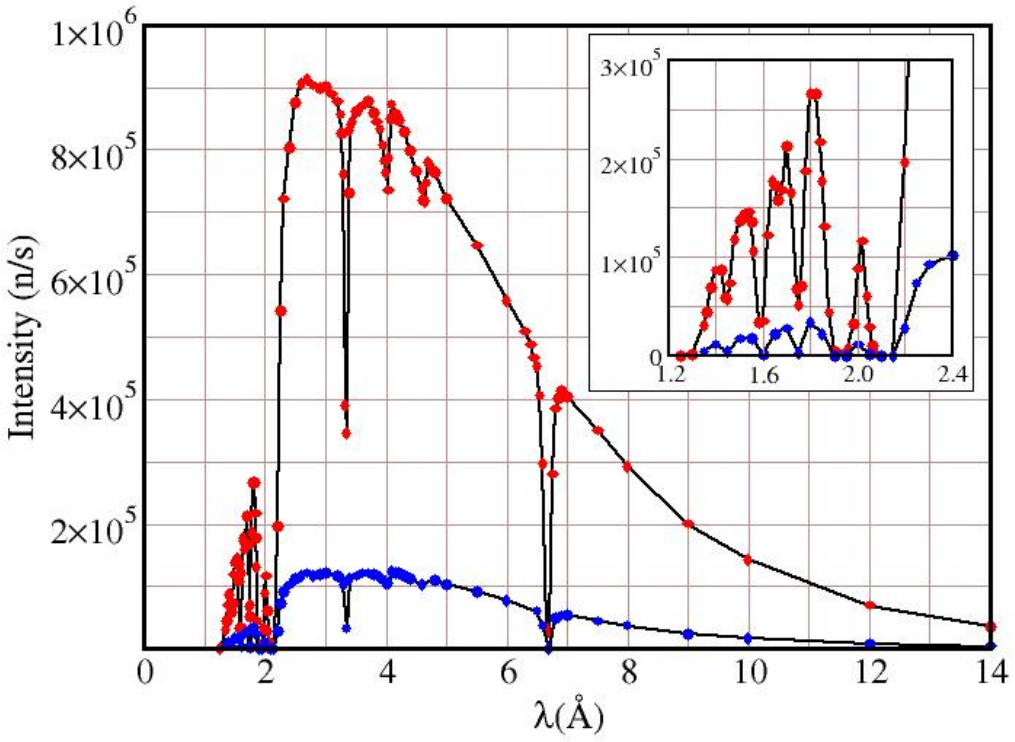

Why are there dips in the measured flux at wavelengths near 3.335 and 6.67 Å?

The resolution of the instrument is approximately triangular and essentially independent of beam height (up to 10 cm) but depends slightly on the width of the beam. Hence samples should ideally be tall and thin rather than short and fat.

The measured elastic energy resolution, for the same choices of chopper slot widths as in the intensity plot above, is shown in the figure below. Lines represent fits to the measurements.

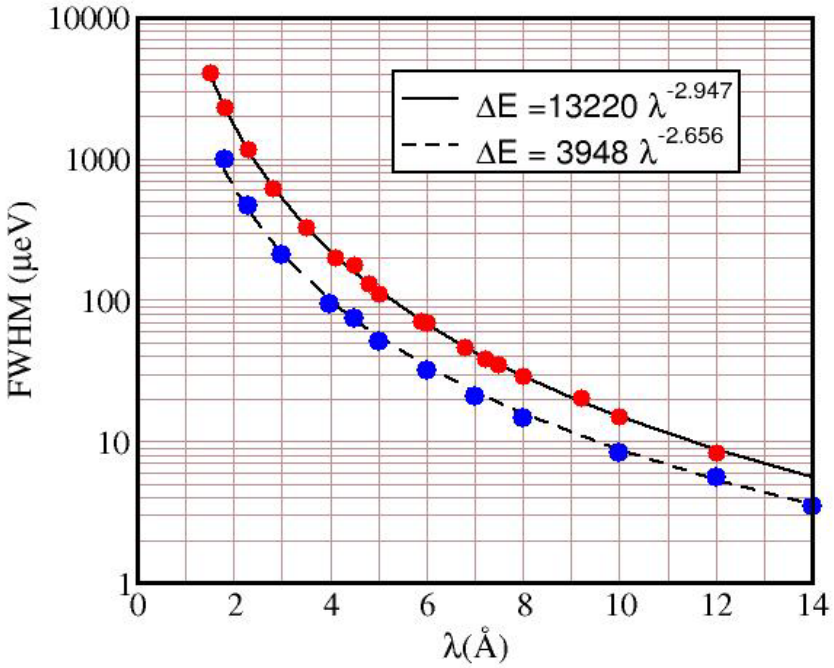

An oscillating radial collimator, inside radius 200 mm, outside radius 300 mm, blade separation 2°, is used to reduce the scattering from sample environment structures.

Can you explain how the radial collimator works, and why it is oscillated?

There are 913 six-atmosphere ^{3}He detectors covering an essentially continuous solid angle of ~0.65 steradians and arranged in three banks:

- Middle bank detector scattering angles range from -30° to -5° and from +5° to +140°
- Upper and lower bank angles range from -30° to -10° and from +10° to +140°

The flight distance from sample to detectors is 4010 mm. The flight chamber is purged with argon.

Why is the flight chamber purged with argon?

Appendix B. Possible Experiments on the Disk Chopper Spectrometer

Phenomena that can be investigated include:

- Translational and rotational diffusion processes, where scattering experiments provide information about time scales, length scales and geometrical constraints; the ability to access a wide range of wave vector transfers, with good energy resolution, is key to the success of such investigations
- Low energy vibrational and magnetic excitations and densities of states
- Tunneling phenomena
- Low Q powder diffraction

Research areas include:

- **Chemistry** --- e.g. clathrates, molecular crystals, fullerenes
- **Polymers** --- bound polymers, glass phenomenon, confinement effects
- **Biological systems** --- protein folding, protein preservation, water dynamics in membranes
- **Physics** --- adsorbate dynamics in microporous/mesoporous systems (MOFs, zeolites, clays etc.) and in confined geometries, metal-hydrogen systems, glasses, magnetic systems
- **Materials** --- negative thermal expansion materials, low conductivity materials, hydration of cement, carbon nanotubes, proton conductors, metal hydrides, hydrogen and methane storage, carbon dioxide capture

Appendix C. Some useful properties and relationships

Neutron properties

Mass:	$m_n = 1.660\times10^{-24}$ g
Electric charge:	0
Spin:	½
Magnetic moment:	-1.913 nuclear magnetons

Exact relationships

$$\lambda = \frac{h}{mv} \qquad E = \frac{1}{2}mv^2 \qquad k = \frac{2\pi}{\lambda}$$

Approximate relationships

$$E[\text{meV}] = \frac{81.8}{(\lambda[\text{Å}])^2}; \quad v[\text{mm}/\mu\text{s}] = \frac{3.956}{\lambda[\text{Å}]}; \quad E[\text{meV}] = 2.07(k[\text{Å}^{-1}])^2; \quad 1\ \text{meV}=8.1\ \text{cm}^{-1}$$

Appendix D. Spin Incoherence

The strength of the scattering of a neutron by a nucleus, i.e. the neutron scattering length, depends on the spin of the compound nucleus. For an isotope with nuclear spin I the combined "nucleus + neutron" spin, I′, has two possible values, $I^+ = I+½$ and $I^- = I-½$, with which we associate two possible scattering lengths b^+ and b^-. Each of the possible values of the combined spin has 2I′+1 possible spin states, i.e. 2(I+½)+1 = 2I+2 and 2(I-½) +1 = 2I states respectively, for a total of 4I+2 spin states.

If the neutron and nuclear spins are randomly orientated, all states are equally probable, and the probabilities of the combined + and - spin states are $p^+ = (I+1)/(2I+1)$ and $p^-=I/(2I+1)$ respectively.

The mean scattering length, <b>, and the mean of the scattering length squared, $<b^2>$,

$$<b> = p^+b^+ + p^-b^- \quad \text{and} \quad <b^2> = p^+(b^+)^2 + p^- (b^-)^2$$

are used to calculate the coherent and incoherent bound cross sections. These cross sections are defined as follows:

$$\sigma_{coh} = 4\pi \langle b \rangle^2 \quad \text{and} \quad \sigma_{inc} = 4\pi \left(\langle b^2 \rangle - \langle b \rangle^2 \right).$$

Working through the numbers for hydrogen and deuterium is instructive. The relevant scattering lengths for hydrogen are $b^+ = 1.086\times10^{-12}$ cm and $b^- = -4.751\times10^{-12}$ cm, whereas the values for deuterium are $b^+ = 0.951\times10^{-12}$ cm and $b^- = 0.095\times10^{-12}$ cm.